processes

MDPI

Article

Effects of Coal Permeability Anisotropy on Gas Extraction Performance

Futian Nian [1,2], Feng Ju [1,*], Chunshan Zheng [3,*], Haifei Wu [3] and Xiaoyu Cheng [4]

[1] State Key Laboratory for GeoMechanics and Deep Underground Engineering, China University of Mining and Technology, Xuzhou 221116, China
[2] China Coal Xinji Liuzhuang Mining Co., Ltd., Fuyang 236200, China
[3] Joint National-Local Engineering Research Centre for Safe and Precise Coal Mining, Anhui University of Science and Technology, Huainan 232001, China
[4] China Coal Energy Research Institute Co., Ltd., Xi'an 710054, China
* Correspondence: jf122106@126.com (F.J.); chunshanzheng@aust.edu.cn (C.Z.)

Abstract: To investigate gas flow characteristics in coal seams with strong anisotropy, a coupled anisotropic dual-porosity model was established. Effects of permeability anisotropy on variations in gas pressure, gas extraction volume and effective extraction areas were analyzed. Furthermore, mechanisms of crustal stress, initial gas pressure, ultimate adsorption strain and Langmuir volume constant on permeability anisotropy and extraction amount were studied. Results show that permeability anisotropy could result in an elliptical pressure drop zone around production boreholes. Changes in effective gas extraction areas are divided into three stages: slow growth in an elliptical shape, rapid growth with a superposition effect and steady growth in a funnel shape. Permeability isotropy enables faster reaching of stage III than the anisotropy case. As the vertical stress increases, gas pressure distribution around boreholes gradually changes from an ellipse with horizontal direction as long axis to a circle. Larger initial gas pressure could bring consistently higher gas production in the initial and middle extraction stages, and a faster decrease in the late phase. When gas pressure is 2.5 MPa, the peak daily gas production in initial extraction stage is about three times higher than that in the late phase. Ultimate adsorption strain is positively correlated with permeability change. This relationship becomes more significant with a longer extraction time. In contrast, permeability variation is inversely proportional to the Langmuir volume constant in the initial extraction stage. However, these factors are directly proportional in the late stage. The order of significance of each factor's effect on permeability is crustal stress > ultimate adsorption strain > initial gas pressure > Langmuir volume constant. Moreover, initial gas pressure has the most significant effect on gas extraction volume, while Langmuir volume constant has the least significant impact. Results could provide a theoretical reference for extraction borehole design and drainage parameter setting to improve extraction performance.

Keywords: gas extraction; permeability anisotropy; effective extraction area; gas pressure; mining safety

Citation: Nian, F.; Ju, F.; Zheng, C.; Wu, H.; Cheng, X. Effects of Coal Permeability Anisotropy on Gas Extraction Performance. *Processes* **2023**, *11*, 1408. https://doi.org/10.3390/pr11051408

Academic Editors: Lei Qin and Ruiyue Yang

Received: 2 April 2023
Revised: 24 April 2023
Accepted: 4 May 2023
Published: 6 May 2023

1. Introduction

With rising coalbed depth, crustal stress, gas pressure and strata temperature are becoming increasingly high. Thus, principal hazards are becoming even more difficult to manage, which is evident, particularly in major coal-production countries, where the coalbed-methane-related incidents account for a large proportion [1,2].

Coal seam gas extraction is a useful method for controlling methane-related incidents [3,4]. Flow of gas is largely controlled via coal permeability. In this regard, scholars have conducted much research on theoretical models of permeability and numerical simulations of multi-field coupled gas flow [5–7]. Most classical permeability models take surface coalbed methane extraction as the research background, and are based on assumptions of constant vertical load, elastic deformation and permeability isotropy. Pore structure

properties and gas migration forms of coal are systematically classified, and gas–solid coupled models are established.

In terms of single-porosity single-permeability models, Yang et al. found that volume strain and permeability showed a positive correlation based on their theoretical relationship [8]. Based on gas seepage and coal deformation theory, Zhang et al. [9] established a mathematical model of flow-solid coupling for coal mine roadway pre-discharge in gas zones. Fan et al. [10] studied the effect of various borehole designs on methane drainage efficiency via constructing a coupled hydraulic–mechanical model. Xu et al. [11] analyzed gas extraction characteristics under multiple stress concentration conditions by establishing a dynamic fluid–solid coupled model, considering plastic and dilatancy deformation. Based on relevant theories, such as seepage mechanics, rock mechanics and heat transfer, Yang et al. [12] established a multi-field coupled thermal–fluid–solid mathematical model of coalbed methane extracted through heat injection, and analyzed the mechanism of the effect of heat injection on gas migration rules. Liu et al. [13] established a permeability model for defining permeability anisotropy evolution induced through gas adsorption in stress state. They found that changes in coal permeability were determined only through changes in gas pore pressure and expansion strain for uniaxial strain constraints and constant volume reservoirs. In both cases, effective stress' impacts were replaced with variations in gas pore pressure and expansion strain. Based on a coupled stress–seepage mathematical model of coal containing gas, Shang et al. [14] investigated the influence of some parameters on the methane extraction radius, concluding that one vital issue for improving methane drainage efficiency is enhancement of initial coal permeability before pre-drainage.

With regard to dual-porosity single-permeability models, to reveal methane flow characteristics around borehole in methane drainage process, Liang et al. [15] investigated borehole spacing's impact on drainage performance in Shaqu Mine by constructing a multi-field coupled stress–diffusion–seepage model. Liu et al. [16] investigated changes in methane pressure and coal permeability using a modified Palmer and Mansouri model. Liu et al. [17] constructed a multi-field coupled model containing methane flow, deformation of coal and gas diffusion, etc. They also investigated the spatio-temporal evolution of physical fields during laboratory and engineering-scale methane flow, and explored the non-Darcy's flow's influence on the methane flow of slotted coal. Li et al. [18] investigated borehole spacing's impact on methane extraction based on a dual media model. Qin et al. [19] developed a coupled model based on dual-porosity single-permeability, using double-permeability theory to reveal enrichment migration law of coal seam gas. Wei et al. [20] obtained a new permeability model, taking shear and normal stresses into account. They created a coupled model with coal deformation, fluid flow and diffusion equations, considering shear dilatancy. Danesh NN et al. [21] found that ignoring the role of creep could seriously overestimate coal permeability. Therefore, a multi-physics coupled model that took into account the creep effect was constructed and applied to evaluate gas extraction performance. Results showed that more than 13% deviation in soft coal occurs if the creep issue is ignored. Zhang et al. [22] studied the mechanism of local–global expansion on permeability, and developed a coupled model considering matrix, fracture, matrix fluid and fracture fluid interactions. Liu et al. [23] studied spatio-temporal methane flow variation in adsorption and desorption processes. They established relationship coupling coal deformation and methane flow models.

Coal is a typical sedimentary rock with developed beddings and joints. Thus, permeability anisotropy of coal seam is a natural characteristic [5,24]. Many previous permeability models were isotropic with single- or dual-porosity structures, ignoring the significant effects of anisotropy. Moreover, there are few investigations on extraction and dynamic seepage changes in borehole groups, making it difficult to guide the scientific layout of boreholes and accurately assess gas extraction.

In this study, based on the matrix (containing pores)–fracture coal structure, a dual-porosity single-permeability coupled model considering permeability anisotropy was established. Flow characteristics of gas extraction largely controlled via anisotropic permeability

were investigated through adopting COMSOL Multiphysics software; investigated factors included the effects of multiple coal factors on permeability anisotropy and extraction performance. The outcomes of this study are expected to guide better arrangement of coal seam boreholes, and enhance safe and efficient gas extraction.

2. Theoretical Modeling

2.1. Physical Model

Methane flow is closely related to pore structure, which is complex and variable in nature. However, in the study of gas migration law, most scholars have simplified the pore structure of coal seams into a homogeneous pore medium model with pure diffusion, a homogeneous fracture medium model with pure seepage, and a pore–fracture dual-medium model with diffusion and seepage. Among them, the dual medium model is recognized and used by many scholars, who believe that coal is composed of coal matrices and staggered fractures. In this study, methane flow was categorized as two phases: the first phase was adsorbed gas migration from coal matrices to fractures (or cleats) in form of Fick diffusion, while the second phase was methane flow in coal fractures following Darcy's flow.

The following assumptions were adopted based on physical coal parameters and gas occurrence and migration features:

Coal could be considered to be a pore–fracture dual-medium model. Meanwhile, methane flow in fractures is only taken into account. Methane migration includes three phases of desorption, diffusion and flow, i.e., a dual-porosity single-permeability system, as shown in Figure 1;
Gas in matrices exists mainly in adsorbed state and is an ideal gas;
Gas in matrices mainly migrates into the fracture via diffusion;
Gas in fracture mostly exists as a free state, ignoring gas on the fracture surface, and fracture seepage follows Darcy's law;
Gas adsorption follows Langmuir adsorption equilibrium equation without considering the temperature effect.

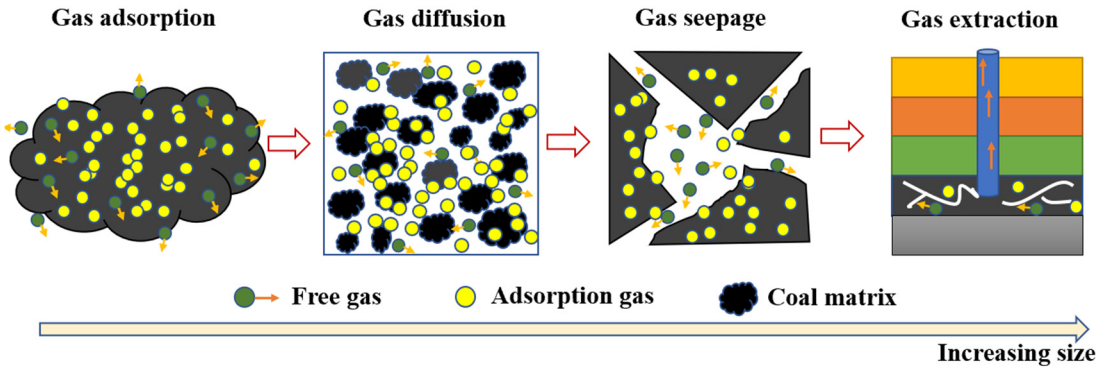

Figure 1. Coal dual-porosity single-permeability system.

2.2. Mathematical Model

2.2.1. Gas diffusion in Coal Matrices

When methane is in dynamic equilibrium state, adsorbed gas pressure in matrices is equal to free gas pressure in fractures. Since adsorbed gas pressure is hardly obtained, its value is generally considered to be equal to gas pressure in fracture at a hypothetical equilibrium corresponding to its state. In a coal matrix, differences in gas concentration results migrate into fractures via Fick diffusion. Based on the law of mass conservation, total desorbed gas and variation in the free-gas amount is equal to diffused gas in fractures.

Methane content within a coal matrix's unit volume includes amounts of adsorbed and free gas:

$$m_m = \frac{V_L p_m}{p_m + P_L} \rho_a \rho_{gs} + \phi_m \frac{M_g}{RT} p_m \tag{1}$$

$$\rho_{gs} = \frac{M_g}{V_m} \tag{2}$$

where V_L represents Langmuir volume constant, m^3/t; ρ_a denotes apparent density of coal, kg/m^3; ρ_m denotes gas density, kg/m^3; P_L denotes Langmuir pressure constant, Pa; M_g represents gas's molar mass, kg/mol; p_m represents gas pressure of matrix, Pa; ϕ_m represents coal matrix's porosity, %; and V_m denotes molar volume of gas under standard conditions, m^3/mol.

State equation for an ideal gas in matrix:

$$\rho_m = \frac{M_g}{RT} p_m \tag{3}$$

Based on mass conservation law [25]:

$$\frac{\partial m_m}{\partial t} = -\frac{M_g}{\tau RT}\left(p_m - p_f\right) \tag{4}$$

Through combining Equations (1)–(4), methane migration equation in coal matrix is as follows:

$$\frac{\partial}{\partial t}\left(\frac{V_L p_m}{P_L + p_m} \rho_a \frac{M_g}{RT_s} p_{gs}\right) + \frac{\partial}{\partial t}\left(\phi_m \frac{M_g}{RT} p_m\right) = -\frac{M_g}{\tau RT}\left(p_m - p_f\right) \tag{5}$$

where τ is gas desorption time, d; R represents gas molar constant, J/(mol·K); p_f denotes gas pressure in fracture, Pa; T is coal seam temperature, K; and T_s represents standard temperature, K.

2.2.2. Gas Flow in Fractures

After borehole extraction breaks the gas pressure equilibrium in coal, gas diffuses into the fracture system from the matrix. The matrix system is equivalent to the fracture system's internal mass source.

Equation of state for an ideal gas in the fracture:

$$\rho_g = \frac{M_g}{RT} p_f \tag{6}$$

Without considering the effect of gravity, Darcy's velocity is [26]:

$$q_g = -\frac{k}{\mu} \nabla p_f \tag{7}$$

According to the law of mass conservation:

$$\frac{\partial}{\partial t}(\phi_f \rho_g) + \nabla \cdot (\rho_g q_g) = Q_m \tag{8}$$

Combining Equations (6)–(8) yields fracture gas flow equation [27,28]:

$$\frac{\partial}{\partial t}\left(\phi_f \frac{M_g}{RT} p_f\right) - \nabla \cdot \left(\frac{M_g p_f}{RT} \frac{k}{\mu_g} \nabla p_f\right) = \left(1 - \phi_f\right) \frac{M_g}{\tau RT}\left(p_m - p_f\right) \tag{9}$$

2.2.3. Anisotropic Permeability Equation

Permeability is an important parameter affecting gas flow. At the same time, it is largely affected by coal pore–fracture features (Figure 2). Firstly, the matrix porosity is [29,30]:

$$\phi_m = \frac{1}{(1+S)}(\phi_{m0}(1+S_0) + \alpha_m(S - S_0)) \tag{10}$$

where $S = \varepsilon_v + \frac{p_m}{K_s} - \varepsilon_s$; $S_0 = \frac{p_{m0}}{k_s} - \varepsilon_s$;

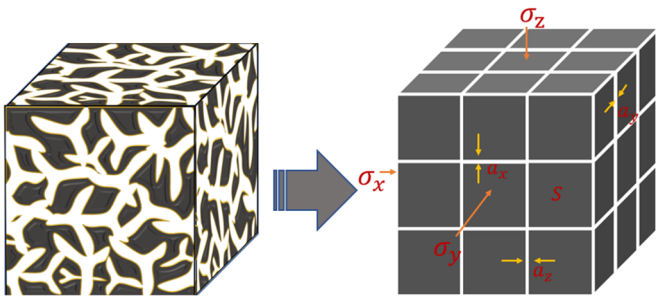

Figure 2. Simplified coal model.

The width of fracture is [31]:

$$a_i = a_{i0} - \Delta a_i = a_{i0} - s(1 - R_m)\left(\Delta\varepsilon_i - \frac{1}{3}\Delta\varepsilon_s\right) \tag{11}$$

where a_{i0} represents initial width of fracture in i direction, m.

Adsorption strain satisfies the Langmuir curve [32,33]:

$$\varepsilon_s = \varepsilon_L \frac{p_m}{p_m + P_L} \tag{12}$$

where ε_L denotes ultimate adsorption strain.

Variation in coal fracture width is:

$$\phi_f \approx \frac{3a}{s} = \frac{3a_i}{s} = \frac{3a_{i0}}{s} - 3(1 - R_m)\left(\Delta\varepsilon_i - \frac{1}{3}\Delta\varepsilon_s\right) \tag{13}$$

According to the initial porosity:

$$\phi_{f0} = \frac{a_{x0} + a_{y0} + a_{z0}}{s} = \frac{3a_{i0}}{s} \tag{14}$$

Porosity of the fracture can be defined as:

$$\phi_f = \phi_{f0} - (1 - R_d)(\Delta\varepsilon_s - \Delta\varepsilon_v) \tag{15}$$

where the volumetric strain is $\Delta\varepsilon_v = \Delta\varepsilon_x + \Delta\varepsilon_y + \Delta\varepsilon_z$.

According to the cubic law of permeability:

$$\frac{k_x}{k_{x0}} = \frac{1}{2}\left[1 - \frac{1}{\phi_{f0}}(1 - R_d)(\Delta\varepsilon_s - 3\Delta\varepsilon_y)\right]^3 + \frac{1}{2}\left[1 - \frac{1}{\phi_{f0}}(1 - R_d)(\Delta\varepsilon_s - 3\Delta\varepsilon_z)\right]^3 \tag{16}$$

Thus, the permeability equation considering anisotropy of coal can be obtained as follows:

$$\frac{k_i}{k_{i0}} = \sum_{i \neq j} \frac{1}{2}\left[1 - \frac{1}{\phi_{f0}}(1 - R_d)(\Delta\varepsilon_s - 3\Delta\varepsilon_i)\right]^3 \tag{17}$$

2.2.4. Coal Deformation Equations

The governing equation of coal stress field, considering matrix pore pressure, fracture fluid pressure, and gas adsorption–desorption, is shown below [29]:

$$\sigma'_{ij} = \sigma_{ij} - \left(\alpha_f P_f + \alpha_m P_m + \frac{K\varepsilon_L P_L}{(P_m + P_L)^2} P_m \right) \delta_{ij} \tag{18}$$

where σ_{ij}' denotes effective stress; δ_{ij} denotes the Kronecker symbol; $\beta_m = (1 - K)/K_m$ represents the effective stress coefficient in fracture, while $\beta_m = K/K_m - K/K_s$ denotes effective stress coefficient in matrix; $K = E/3(1 - 2v)$ represents coal bulk modulus, MPa; $K_m = E_m/3(1 - 2v)$ denotes coal matrix bulk modulus, MPa; σ_{ij} represents total stress; K_s represents bulk modulus of the coal skeleton, MPa; E denotes coal elastic modulus, MPa, while E_m represents coal matrix elastic modulus, MPa; and v represents Poisson's ratio [17].

Constitutive equation of coal is:

$$\sigma'_{ij} = \lambda\delta_{ij}\varepsilon_v + 2G\varepsilon_{ij} \tag{19}$$

where ε_{ij} is the strain tensor; $\lambda = 2G/(1 - 2v)$ denoting Lame constant; $G = E/(2 + 2v)$ represents coal shear modulus, MPa; and ε_v denotes coal volumetric strain.

Gas-containing coal's stress balance equation is:

$$\sigma_{ij,j} + F_i = 0 \tag{20}$$

Meanwhile, its geometric equation is:

$$\varepsilon_{ij} = \frac{1}{2}(u_{i,j} + u_{j,i}) \tag{21}$$

Combining Equations (18)–(21) yields the governing equation of coal deformation:

$$Gu_{i,jj} + \frac{G}{1 - 2v} u_{j,ji} - \alpha_m p_{m,i} - \alpha_f p_{f,i} - K\varepsilon_{s,i} + F_i = 0 \tag{22}$$

Based on the above theoretical model analysis, the multi-field coupling relationship between gas diffusion, seepage and coal deformation is shown in Figure 3. These equations were resolved using the PDE module of COMSOL Multiphysics software to analyze flow properties of gas extraction under the influence of permeability anisotropy.

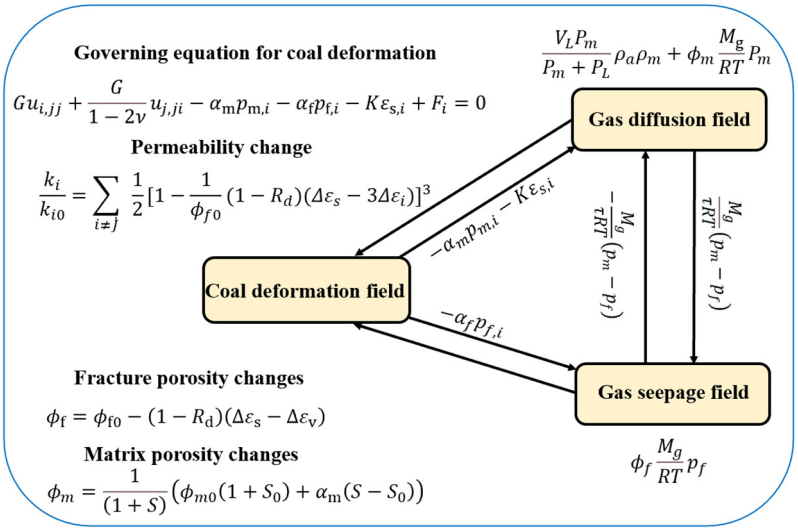

Figure 3. Illustration of multi-field coupling diagram.

3. Numerical Simulation Analysis

The numerical simulation model was established based on field parameters of in-seam borehole drainage and outburst elimination in the targeted mine. The numerical model includes roof strata, floor strata and the coal seam. Three extraction boreholes are located in middle of the coal seam, with a spacing of 5 m and a radius of 0.1 m. The vertical overlying stress is set at the model's top, with a fixed boundary at the bottom and roller support boundaries on both sides. Gas only migrates within coal, and the outside of coal is an impermeable boundary. Dirichlet boundary is used for the borehole boundary. Additionally, because of the strong influence of negative extraction pressure, adsorbed gas pressure at borehole walls is considered equal to gas pressure in fracture. Meanwhile, the diffusion and seepage equations have the same fixed pressure boundary at the borehole wall. The initial displacement of the model is 0. Detailed model settings and parameters are shown in Figure 4 and Table 1.

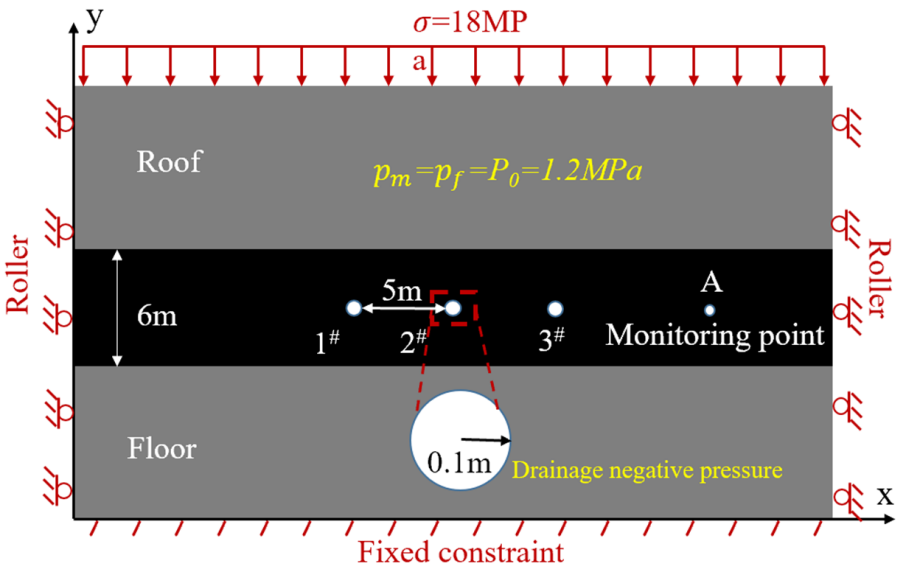

Figure 4. Description of numerical simulation model.

Table 1. Parameter values of numerical simulation model.

Parameter	Value
Coal elastic modulus (MPa)	2713
Elastic modulus of coal matrix (MPa)	8400
Poisson's ratio	0.339
Coal matrix porosity	0.06
Coal fracture porosity	0.012
Gas dynamic viscosity (Pa·s)	1.08×10^{-5}
Initial horizontal permeability (m^2)	1.645×10^{-16}
Initial vertical permeability (m^2)	0.769×10^{-16}
Initial gas pressure (MPa)	1.2
Drainage negative pressure (kPa)	13
Langmuir volume constant (m^3/kg)	0.036
Ultimate adsorption strain	0.012
Langmuir pressure constant (Pa)	1×10^6
Geothermal temperature (K)	293
Coal apparent density (kg/m^3)	1350
Adsorption time (d)	9.2

4. Results Analysis and Discussion

4.1. Effects of Permeability Anisotropy on Extraction Process

(1) Gas pressure distribution

Due to coal structure's anisotropy, permeability is also characterized by anisotropy. In this study, the effects of three different initial permeability anisotropy ratios (Table 2) on gas pressure changes during extraction were analyzed.

Table 2. Simulation schemes for different initial permeability anisotropy ratios.

Case	$k_{x0}(10^{-16}$ m$^2)$	$k_{y0}(10^{-16}$ m$^2)$	k_{x0}:k_{y0}	Drainage Time (Day)
1	1.645	1.645	1:1	
2	4.935	1.645	3:1	200
3	14.805	1.645	9:1	

Analysis outcomes are shown in Figure 5. The pressure contour of gas in coal is not circular but shows a certain elliptical shape while initial permeability is isotropic. The pressure performance on monitoring line is $P_{ab} > P_{ac}$, which results from the difference in stress conditions in the direction perpendicular to those two monitoring lines. The direction perpendicular to the monitoring line segment *ab* is the stress effect of overlying strata. The direction vertical to monitoring line segment *ac* is the roller support boundary. Fracture is more likely to be compressed along *ab* direction, causing a reduction in permeability and difficulty in gas migration. This phenomenon indicates that stress anisotropy can lead to anisotropic characteristics of gas extraction in the case of an isotropic initial permeability of coal. Through comparing Figure 5b with Figure 5a, it is seen that as anisotropy ratio increases, gas pressure behaves as $P_{ab} < P_{ac}$. According to Figure 5c, gas pressure in the horizontal monitoring line *ab* gradually decreases as the anisotropy ratio increases. In Figure 5d, gas pressure shows an increase, followed by a decrease. The reason for this result is that as initial permeability anisotropy ratio increases, the elliptical shape presented during gas extraction becomes narrower in the *ab* direction, and gas in the *ac* direction is more likely to transfer to the dominant flow direction (*ab*), causing a smaller gas pressure at k_{x0}:k_{y0} = 9:1 than k_{x0}:k_{y0} = 1:1 in the monitoring line *ac*.

Figure 6 depicts analysis based on a gas pressure isobaric surface of 0.46–0.75. After 10 d of gas extraction, due to coal initial permeability anisotropy ($k_{x0} = 1.645 \times 10^{-16}$ m^2, $k_{y0} = 0.769 \times 10^{-16}$ m^2), gas pressure contours around borehole show an elliptical pressure drop zone, with the long axis in horizontal permeability direction and the short axis in vertical permeability direction. With the increasing extraction time, the elliptical pressure drop area gradually spreads to the coal boundary. However, influenced by coal thickness, the expansion in vertical direction will not continue after reaching the roof and floor, while the expansion in horizontal direction is accelerated, forming lantern- and funnel-shaped pressure drop zones in turn.

Figure 7 shows that at 10 d of extraction, gas pressure around three boreholes is only partially below 0.74 MPa, with no reduction in gas pressure at locations further away from the boreholes. After 300 d of extraction, gas pressure around those three boreholes is reduced to below 0.74 MPa. The above phenomena indicate that gas pressure is positively related to the distance to the borehole center. This result is because construction of the borehole destroys the initial stress state and forms pressure relief areas around the borehole. Meanwhile, the permeability of coal increases within this area. At a high gas pressure gradient when extraction starts, the gas pressure in the coal seam within this range decreases at a fast rate. Moreover, two variation conditions, namely gas pressure when considering permeability anisotropy ($k_x \neq k_y$, $k_{x0} = 1.645 \times 10^{-16}$ m^2, $k_{y0} = 0.769 \times 10^{-16}$ m^2) and when not considering it ($k_x = k_y$, $k_{x0} = k_{y0} = 1.645 \times 10^{-16}$ m^2), were compared. Influenced by the difference in permeability in the vertical direction, the overall gas pressure, when permeability anisotropy is considered, is greater than when it is not considered.

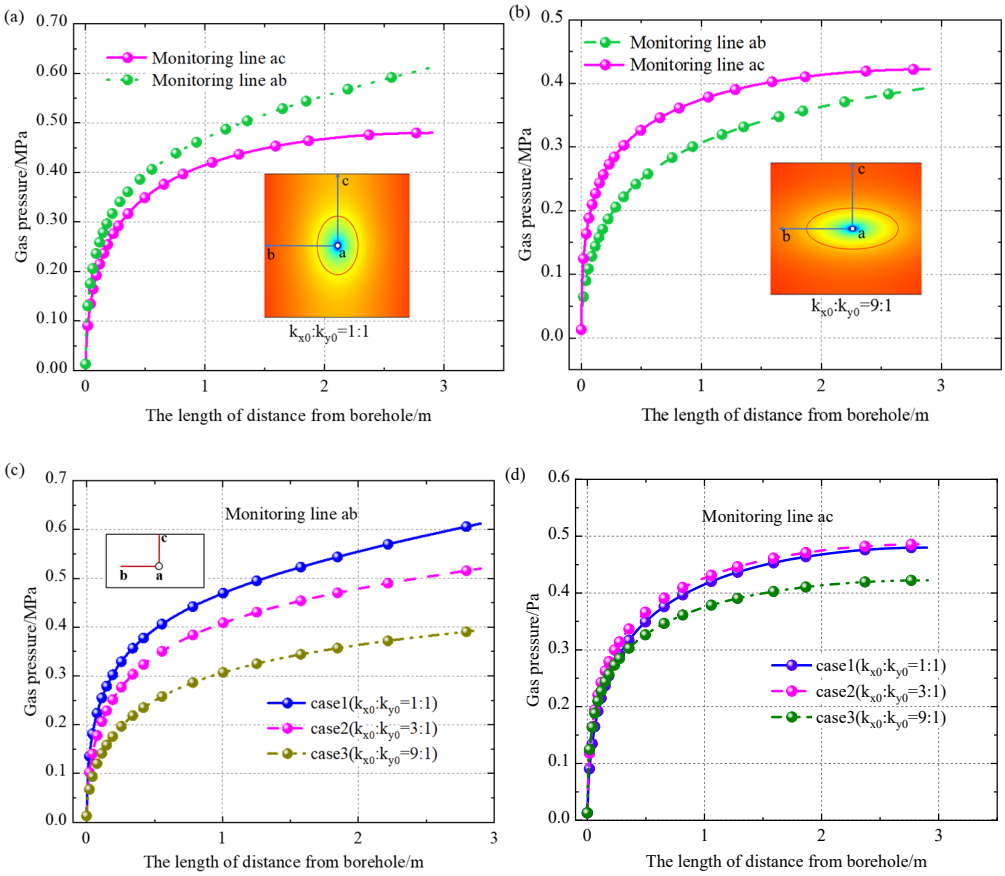

Figure 5. Initial permeability anisotropy ratio's impact on gas pressure change. (**a**) Gas pressure on line ab and line ac (k_{x0}:k_{y0} = 1:1); (**b**) gas pressure on line ab and line ac (k_{x0}:k_{y0} = 9:1); (**c**) gas pressure on line ab (k_{x0}:k_{y0} = 1:1, 3:1 and 9:1, respectively); and (**d**) gas pressure on line ac (k_{x0}:k_{y0} = 1:1, 3:1 and 9:1, respectively).

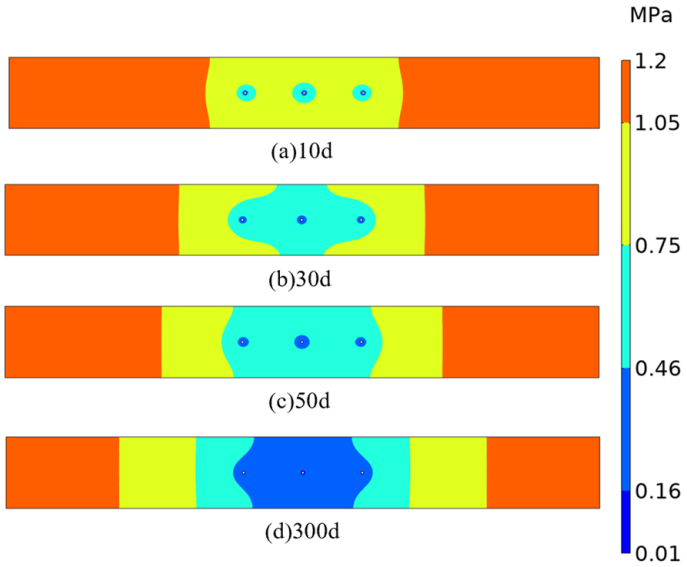

Figure 6. Gas pressure contour map. (**a**) 10 d of drainage; (**b**) 30 d of drainage; (**c**) 50 d of drainage; and (**d**) 300 d of drainage.

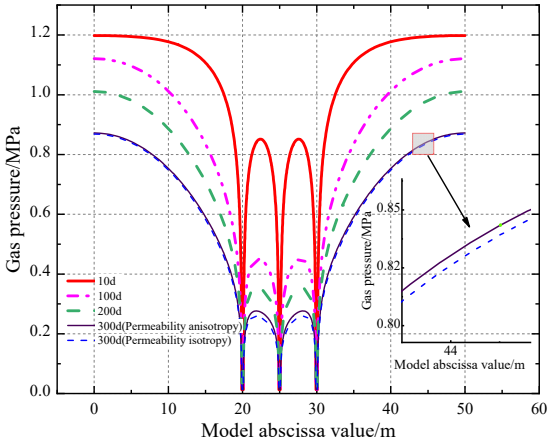

Figure 7. Variations of gas pressure around borehole.

In addition, the gas pressure elevation diagram in Figure 8 (k_{x0} = 1.645 × 10^{-16} m^2, k_{y0} = 0.769 × 10^{-16} m^2) indicates that overall gas pressure reduces with extraction time. Gas pressure is 0.88 MPa at 300 d, even at the farthest point from the borehole. The gas pressure drop rate around the borehole keeps decreasing for two reasons. One reason is that as extraction progresses, the gas pressure gradient and extraction flow dynamic gradually decrease. The other reason is that the decreasing gas pressure and increasing effective stress on coal with time lead to the compression of pores and fractures within coal, and a decrease in permeability. After a period of extraction, the reduced gas content results in matrix shrinkage, which causes fracture opening to increase and permeability to increase again. However, this trend shows limited impact on improving gas extraction efficiency in later stages.

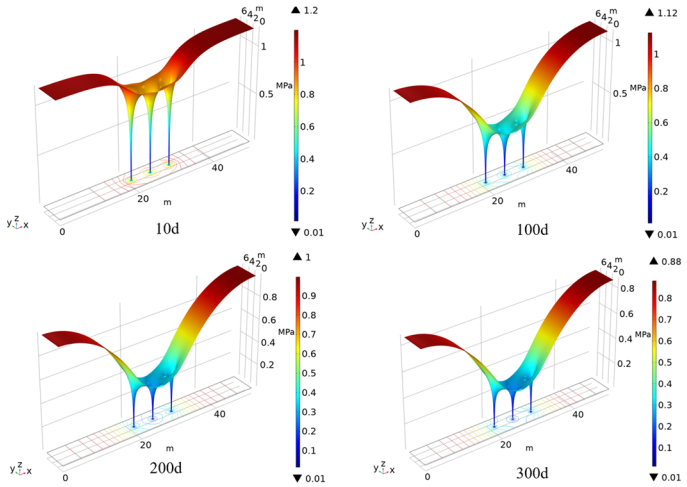

Figure 8. Elevation map of gas pressure distribution.

(2) Changes in gas extraction amount

Deep coal seams experienced high crustal stress environment for a long time due to weight from the overlying strata, which causes fractures closure, resulting in smaller permeability than shallow coal seams. In addition, differences between horizontal and vertical permeability largely affects the gas extraction amount. As shown in Figure 9, when vertical permeability is kept constant of 0.769 × 10^{-16} m^2, the gas extraction amount rises significantly with increase in horizontal permeability. A small increase in horizontal permeability significantly boosts gas production. While horizontal permeability is 2.545 × 10^{-16} m^2, the peak drainage rate increases by about 30 m^3/day compared with the horizontal permeability of 1.645 × 10^{-16} m^2.

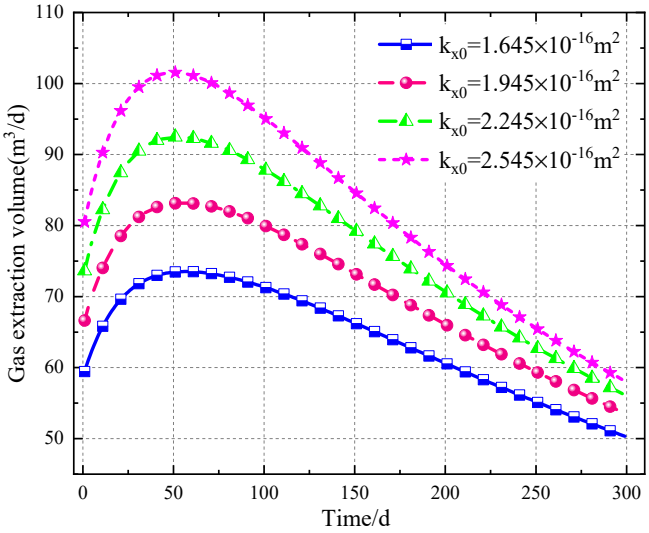

Figure 9. Changes in gas extraction amount corresponding to different horizontal permeability levels.

When horizontal permeability is 1.645×10^{-16} m^2, the increase in vertical permeability only significantly affects the extraction yield at the initial stage of extraction (approximately 100 d) (Figure 10). As extraction continues, this effect decreases. Meanwhile, the greater the vertical permeability level, the smaller the differences between gas extraction volumes. For example, when vertical permeability rises from 0.769×10^{-16} m^2 to 1.669×10^{-16} m^2, peak extraction volume differs by about 10 m^3/d in the first 100 d of extraction, while the daily extraction volume is basically the same at about 300 d of extraction. This result is because, at the initial extraction stage, the crustal stress significantly affects extraction permeability, and reservoirs with high initial vertical permeability have a large pressure drop and fast gas desorption. However, as time increases, the shrinkage effect of the coal matrix becomes an important factor affecting permeability and the volume of gas extracted. Therefore, the permeability in the horizontal direction is a key factor in controlling the amount of gas extracted from boreholes in this model. Additionally, for both horizontal and vertical permeabilities, the daily extraction rate increases to the peak before a decrease (larger permeability could shorten the time required to reach peak value). For instance, at a vertical permeability of 0.769×10^{-16} m^2 and a horizontal permeability of 1.645×10^{-16} m^2, the extraction rate increases from 59 m^3/d to a peak of 73 m^3/d at about 50 d during the initial stage. However, after 50 d, the daily extraction volume decreases day by day and drops to 50 m^3/d at about 300 d.

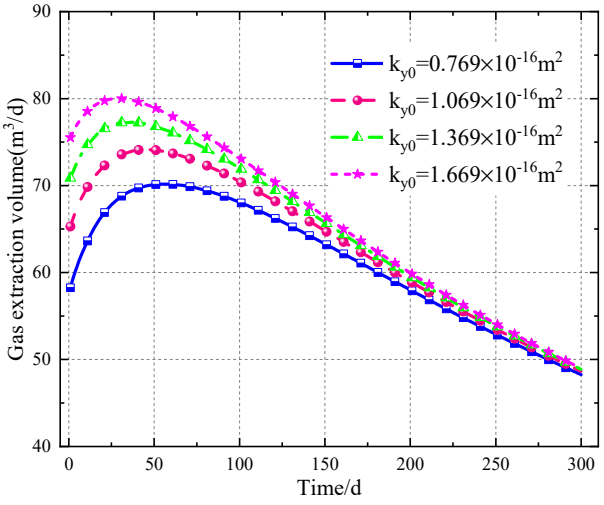

Figure 10. Changes of gas extraction amount corresponding to different vertical permeability levels.

(3) Effective gas extraction area

According to relevant regulations on gas extraction [25,34], coal seam gas pressure should be decreased to less than 0.74 MPa if there is no gas pressure value at the coal seam's original outburst depth, or the pre-drainage rate of gas in coal should be more than 30%. The locations at which the extraction rates of gas reach 10% and 30% are taken as the influence radius (R_2) and effective radius (R_1) of borehole for gas extraction, respectively (Figure 11). Although scholars previously conducted numerous studies about boreholes' effective drainage areas, the effect of permeability anisotropy was rarely considered. As shown in Figure 12, the effective extraction range, taking the effect of permeability anisotropy into account ($k_x \neq k_y$, $k_{x0} = 1.645 \times 10^{-16}$ m^2, $k_{y0} = 0.769 \times 10^{-16}$ m^2), is an ellipse with OB as the long axis and OA as the short axis. In the case of isotropic permeability ($k_x = k_y$, $k_{x0} = k_{y0} = 1.645 \times 10^{-16}$ m^2), it is generally a circle with OB as the radius. The ranges of effective extraction area are basically the same in direction, being parallel with the coal bedding; however, they significantly differ in direction when vertical to the bedding.

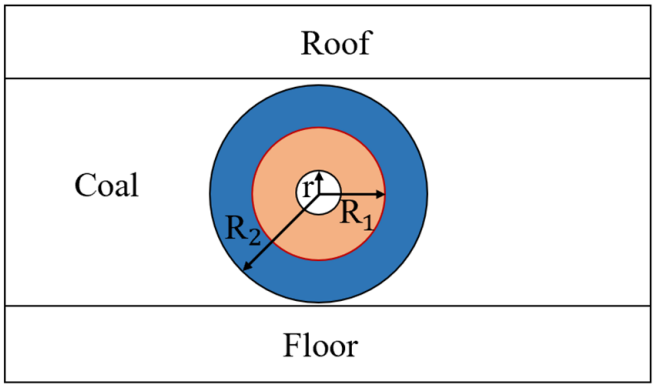

Figure 11. Gas extraction area of borehole.

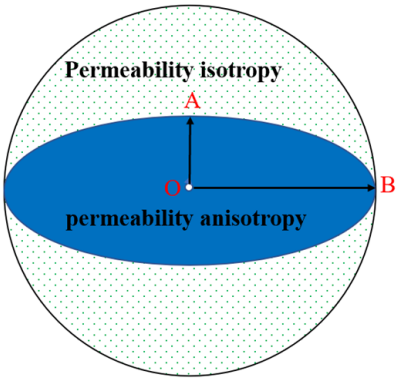

Figure 12. Borehole effective extraction area considering permeability anisotropy and not.

Most deep coal seams in coal mines are anisotropic. If borehole arrangement is guided using research results for the isotropic coal seam, there will be lots of ineffective extraction areas, which will cause high residual gas content in some areas of coal seam, thereby threatening the safe production of an underground coal mine. Therefore, to eliminate this potential risk factor, anisotropic characteristics of coal seams should be considered for borehole arrangement in deep coal seams. Since the extraction area affected through anisotropy is irregular, the following method is proposed to calculate the effective extraction area:

$$S = \iint_D f(x, y) d\sigma \tag{23}$$

where S is the effective extraction area, m^2; and x and y are the locations in the model where gas pressure is below 0.74 MPa or equivalent, m.

As shown in Figure 13, at the same crustal stress (18 MPa), the change in the effective extraction area of the three-boreholes group is categorized into three phases. Phase I: three independent boreholes do not interact each other, and the effective extraction area grows in an ellipse. At this time, the superposition effect of multiple boreholes has not yet occurred, and the effective extraction area increases slowly. Phase II: borehole interaction starts to occur, the effective extraction area of extraction overlaps, and gas extraction efficiency improves. Gas pressure around borehole 2 is below 0.74 MPa for a shorter period. The effective extraction area grows faster, indicating that the rate of gas pressure drop at this time is proportional to the strength of the superposition effect. Phase III: although still affected through the superposition effect, the area around the middle borehole is already below 0.74 MPa. At this time, mainly influenced by the left and right boreholes, the increase in the effective extraction area gradually becomes steady.

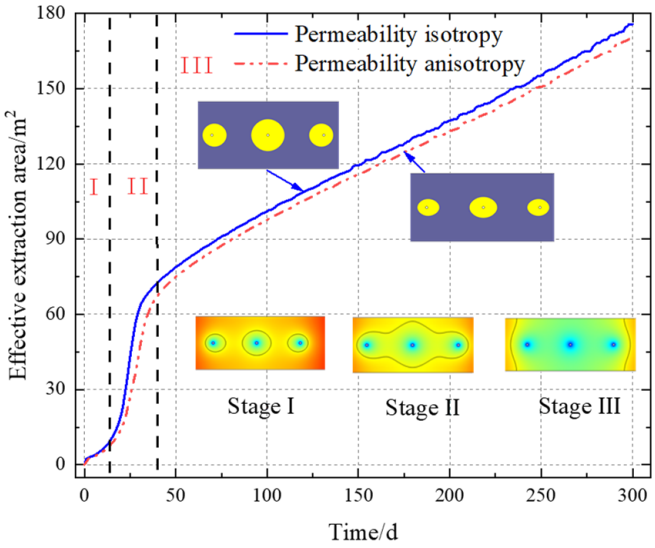

Figure 13. Changes in effective extraction area.

Moreover, permeability isotropy enables a faster occurrence of stage III than anisotropy. The reason for this result is that when considering permeability anisotropy, the permeability in the vertical direction is low, which poses difficulty for gas migration and makes the gas pressure drop more slowly. Thus, stage III is entered more quickly when permeability is isotropic.

The thickness of the coal seam is a major parameter affecting the effective extraction area, the results of which are shown in Figure 14. Variation in the thickness of coal seams shows no impact on overall changing trend of extraction area. In stages I and II, the effective extraction area is inversely proportional to coal seam thickness. Effective extraction area increases fastest when the thickness is 6 m, and the corresponding area value is the smallest at 12 m. The growth rate of the effective extraction area from large to small is 6 m, 8 m, 10 m and 12 m, respectively. The effective areas corresponding to coal thicknesses of 6 m, 8 m, 10 m and 12 m enter stage III at about 37 d, 58 d, 84 d, and 125 d, respectively. After reaching stage III, the growth rates of the extraction range corresponding to those four coal thicknesses tend to be identical. At this stage, the effective area shows a positive relationship with coal seam thickness. The thicker the coal seam, the bigger the effective drainage area.

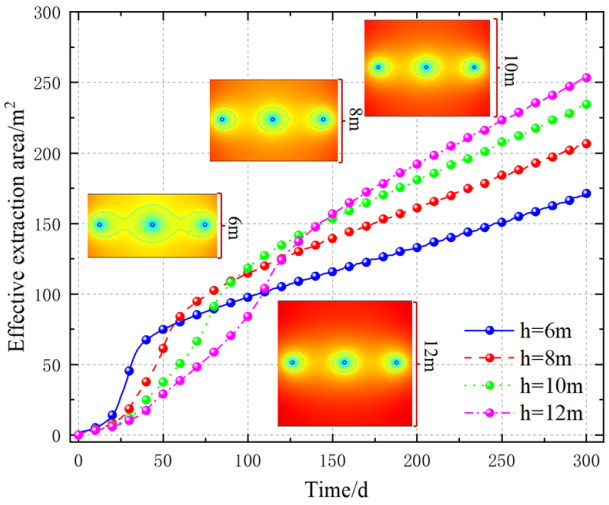

Figure 14. Effective extraction area variations corresponding to four coal seam thicknesses.

4.2. Effect Analysis of Multiple Factors on Permeability Anisotropy and Extraction Volume

Effects of crustal stress, ultimate adsorption strain, initial gas pressure and Langmuir volume constant on permeability anisotropy and extraction volume were investigated in detail in this section. Since the horizontal permeability mainly controls gas extraction performance in this model, analysis of impact of each parameter on horizontal permeability was primarily focused on:

(1) Crustal stress

To explore impact of different crustal stresses on gas extraction, vertical crustal stresses of 10 MPa, 14 MPa, 18 MPa and 23 MPa were applied. In Figure 15, the range and magnitude of gas pressure drops become smaller as the crustal stress increases during the same extraction time (15 d). Additionally, the difference between horizontal and vertical permeability (k_{x0} = 1.645 × 10^{-16} m^2, k_{y0} = 0.769 × 10^{-16} m^2) causes different gas pressures at each location, and the pressure contour map shows an elliptical shape. However, with the increasing crustal stress, gas pressure distribution around the borehole gradually changes from an ellipse with the horizontal direction as long axis to a circle. This result is because effective stress acting on the vertical coal seam direction rises when crustal stress expands. As a result, horizontal fracture opening and horizontal permeability decreases and gas flow capacity weakens, indicating that the dominant gas flow direction changes with crustal stress and other effects.

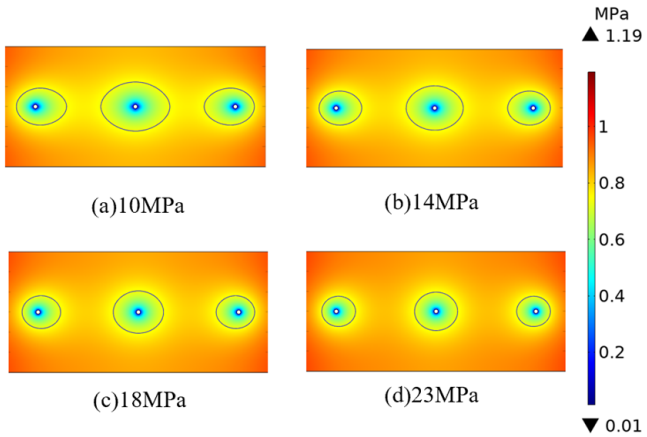

Figure 15. Variation nephogram of gas pressure under different ground stresses. (**a**) 10 MPa of stress; (**b**) 14 MPa of stress; (**c**) 18 MPa of stress; and (**d**) 23 MPa of stress.

As shown in Figure 16a, volumetric strain of coal increases with the increasing crustal stress, causing porosity and fracture permeability to decrease. Taking point A in the numerical model as an example, horizontal permeability at this point decreases with increasing ground stress and increases with extraction time. At the initial extraction stage, when crustal stress increases from 10 MPa to 23 MPa, the proportion of change in permeability at point A decreases from 0.9508 to 0.5759 compared to initial permeability. The variation is as high as 39.4%, which indicates that horizontal permeability is significantly reduced, causing difficulties in gas migration. As a result, gas extraction volume becomes lower, and gas production takes longer to reach the peak. In addition, daily gas production decreases with increasing crustal stress. Gas production reaches the maximum at the crustal stress of 10 MPa. The peak gas production is 83 m^3/d, 76 m^3/d, 71 m^3/d and 66 m^3/d at about 50 d for crustal stresses of 10 MPa, 14 MPa, 18 MPa and 23 MPa, respectively.

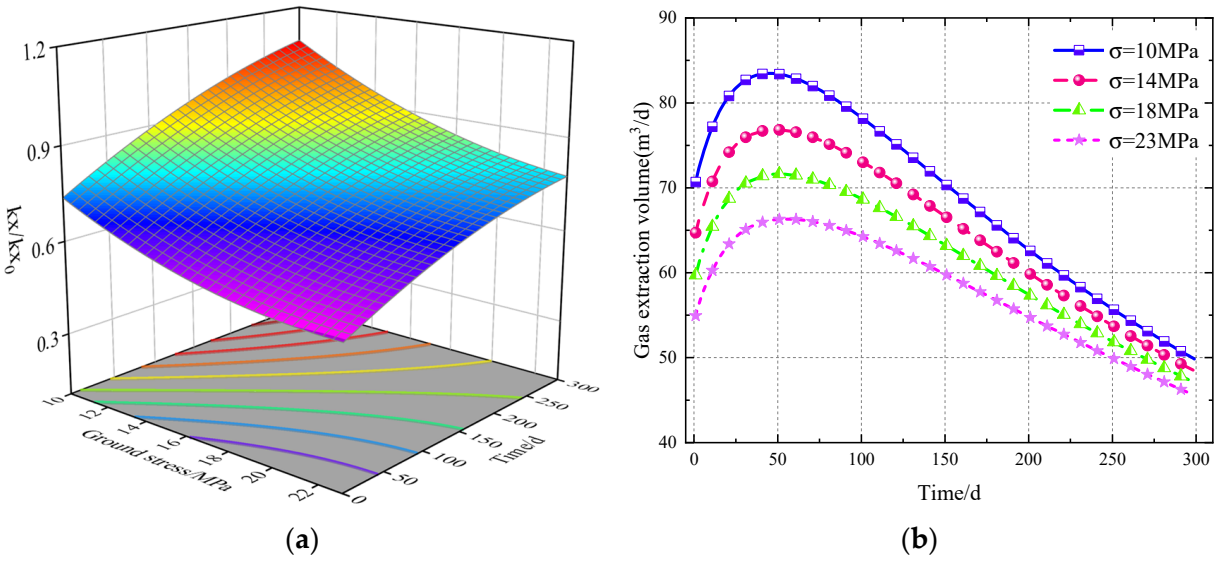

Figure 16. Variation in permeability and gas extraction amount at point A under different ground stresses. (**a**) Change in horizontal permeability at point A; and (**b**) change in gas extraction volume.

(2) Ultimate adsorption strain

Variations in horizontal permeability and gas extraction volume at point A corresponding to different ultimate adsorption strain ε_L values is shown in Figure 17. As shown in Figure 17a, horizontal permeability at point A varies little, with different ultimate adsorption strain ε_L in initial extraction phase. Changes in the permeability of point A increase with ultimate adsorption strain ε_L with longer extraction times. At 300 d of extraction, the change in permeability of point A (ε_L = 0.016) increases by 27.5% compared to the case of ε_L = 0.004, indicating a significant increase in permeability. Figure 17b shows the amount of extracted gas at different moments. An increase in ε_L causes increased permeability and promotes gas migration in a coal seam. When ε_L is 0.016, the maximum gas production is 80 m^3/d. When ε_L = 0.004, the peak gas extraction volume is 61 m^3/d. A gas pressure drop in coal fractures promotes gas desorption from the matrix and causes matrix shrinkage. Matrix shrinkage results in an increase in horizontal permeability. Therefore, compared with the case of ε_L = 0.004, the gas adsorption amount at ε_L = 0.016 is large, and matrix shrinkage takes a longer time, resulting in it taking longer to reach the extraction peak value.

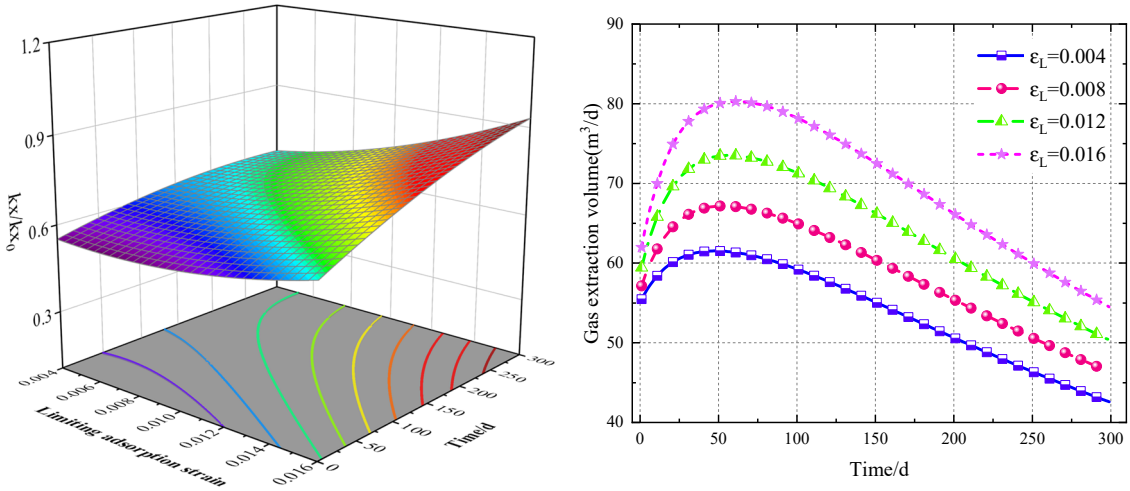

(**a**) (**b**)

Figure 17. Variation in permeability and gas extraction amount at point A under different ε_L. (**a**) Change in horizontal permeability at point A; and (**b**) change in gas extraction volume.

(3) Initial gas pressure

Initial gas pressure mainly causes a change in permeability through affecting effective stress at the initial drainage phase. Higher initial coal seam gas pressure could lower effective stress, resulting in higher horizontal permeability. As shown in Figure 18a, the change in horizontal permeability at point A increases with increasing initial gas pressure. At 300 d of extraction, variation in permeability at point A when p0 = 2.5 MPa increases by 46.7% compared to the case of p0 = 1.2 MPa. Figure 18b indicates that at the initial drainage phase, maximum daily gas production is 73 m^3/d, 112 m^3/d, 193 m^3/d and 292 m^3/d when p0 = 1.2 MPa, p0 = 1.5 MPa, p0 = 2.0 MPa and p0 = 2.5 MPa, respectively. Higher initial coal seam gas pressure results in a shorter drainage time to reach peak gas production. Moreover, the shrinkage effect of a matrix in the middle stage of extraction becomes significant with time. As a result, permeability increases significantly, resulting in continued high gas production in the initial and middle stages. In contrast, the extraction volume in the late stage decreases rapidly. This phenomenon is most evident at p0 = 2.5 MPa, where the peak amount of daily gas extraction is about three times the minimum value at the late stage.

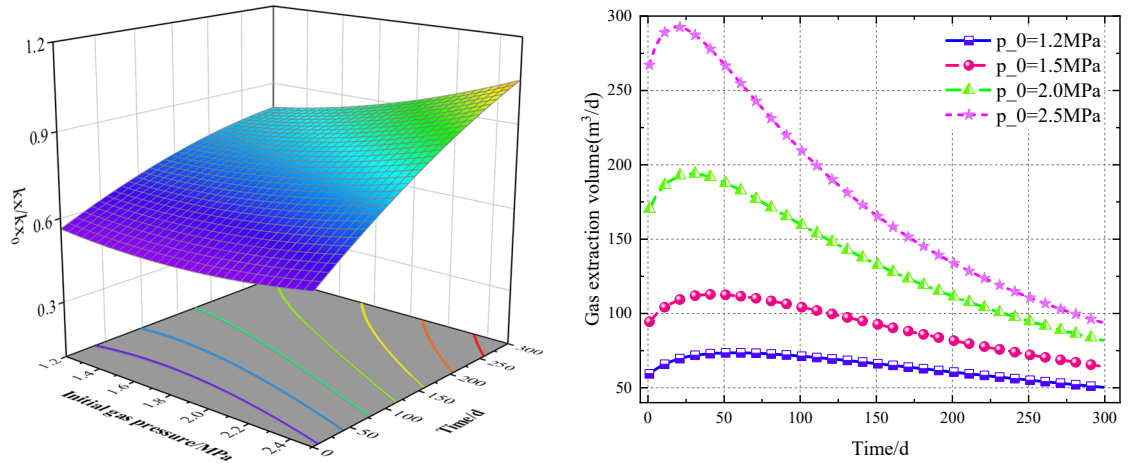

(**a**) (**b**)

Figure 18. Variation in permeability and gas extraction amount at point A under different initial gas pressures. (**a**) Change in horizontal permeability at point A; and (**b**) change in gas extraction volume.

(4) Langmuir volume constant

As Langmuir volume experiences a constant increase, gas content adsorbed in coal matrix also increases, while permeability decreases. As shown in Figure 19a, the proportion of change in horizontal permeability at point A decreases with increasing Langmuir volume constant, i.e., the permeability value becomes smaller, but increases with extraction time. Lowered permeability makes it difficult for gas to migrate in a coal seam, resulting in low daily production in the initial extraction stage and a delayed time required to reach the peak (Figure 19b). Therefore, when V_L is 0.040 m^3/kg, the daily extraction peak arrives the latest. Meanwhile, the daily extraction volume remains the smallest in the initial stage of extraction. However, after reaching the peak of daily gas production, daily gas production increases significantly, with the increasing Langmuir volume being constant. The extraction amount in the late stage is opposite to that in the initial stage, i.e., the corresponding daily extraction volume is the minimum when V_L is 0.025 m^3/kg (not 0.040 m^3/kg). This finding mainly results from the following two causes: (i) during initial gas extraction, the reservoir pressure does not drop below the critical desorption pressure, making desorption difficult. Extracted gas is mainly free gas. However, the differences in pressures in fracture and matrix rise with longer extraction time, resulting in accelerated matrix desorption (the source of extracted gas). Therefore, bigger V_L could bring higher daily gas production in later stage; and, (ii) for coal with larger V_L, the shrinkage effect of the matrix in the late stage of extraction is also greater, causing a significant increase in permeability and a higher daily extraction volume.

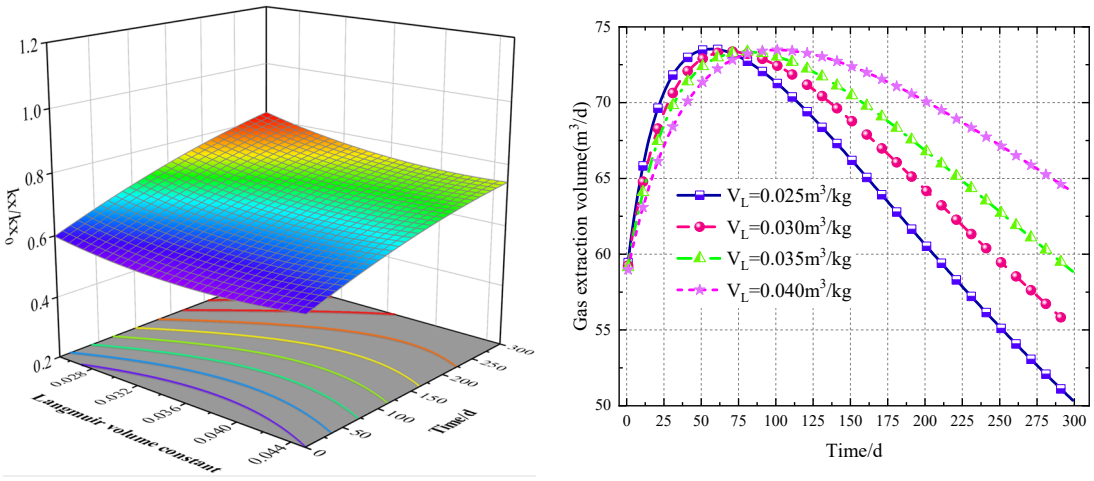

(**a**) (**b**)

Figure 19. Variation in permeability and gas extraction amount at point A under different Langmuir volume constants (V_L). (**a**) Change in horizontal permeability at point A; and (**b**) change in gas extraction volume.

Variance analysis results regarding the effects of the above parameters on horizontal permeability are shown in Table 3.

Table 3. Analysis of variance.

Factor	*F*-Value	*p*-Value	R^2	Significance
Crustal stress (σ)	45.06	0.0003	0.9629	√
Ultimate adsorption strain (ε_L)	14.63	0.0065	0.9105	√
Initial gas pressure (p0)	8.50	0.0388	0.9466	√
Langmuir volume constant (V_L)	1.72	0.2308	0.9355	×

Note: $p < 0.05$ represents significance. *p*-value is influenced by determination coefficient R^2 and *F*-value.

According to the above table, the significance order of effect of each factor on variation in horizontal permeability is crustal stress > ultimate adsorption strain > initial gas pressure > Langmuir volume constant. The impact of crustal stress on variation in horizontal permeability is the most significant factor. From the perspective of gas extraction amount, the significance order of those four factors' effects is initial gas pressure > crustal stress > ultimate adsorption strain > Langmuir volume constant. The initial gas pressure is also the most significant parameter affecting gas drainage amount.

5. Conclusions

(1) Affected by permeability anisotropy, elliptical pressure drop regions are formed around boreholes. Meanwhile, with an increasing anisotropy level, gas pressure keeps decreasing in the horizontal direction, while it increases before dropping in the vertical direction. Changes in effective gas extraction areas have three stages: slow growth in an elliptical shape, rapid growth with a superposition effect, and steady growth in a funnel shape. Coal seam thickness mainly affects stage II. The effective extraction area is inversely related to coal seam thickness at stages I and II, while these factors are directly proportional in stage III.

(2) As vertical crustal stress increases, the range and magnitude of gas extraction pressure drop become smaller. Gas pressure distribution around boreholes gradually changes from an ellipse with the horizontal direction as long axis to a circle. When crustal stress rises from 10 MPa to 23 MPa, permeability increases at the monitoring point before decreasing by 39.4%. The peak daily gas extraction volume decreases from 83 m^3/d to 66 m^3/d, with a longer time to peak value.

(3) Ultimate adsorption strain has little effect on permeability variation in the initial drainage stage. As the extraction continues, rising permeability with increasing ultimate adsorption strain becomes significant, as does the gas extraction volume. Higher initial gas pressure could result in permeability rising, thus shortening the extraction time needed to reach peak gas production. Meanwhile, gas production remains high in the initial and middle stages of extraction and decreases rapidly in the late stage. Permeability change is inversely proportional to Langmuir volume constant in the initial extraction stage. Higher Langmuir volume constant results in lower daily gas production and a delayed time to peak. However, after reaching the peak production value, permeability variation in the late stage is proportional to Langmuir volume constant.

(4) The significance order of each factor's effect on permeability variation is as follows: crustal stress > ultimate adsorption strain > initial gas pressure > Langmuir volume constant. Above results could provide a theoretical reference for gas drainage borehole design and drainage parameter setting to enhance drainage performance.

Author Contributions: Conceptualization, F.N. and C.Z.; Formal analysis, F.N.; Funding acquisition, C.Z.; Investigation, H.W.; Methodology, F.J. and H.W.; Project administration, X.C.; Resources, X.C.; Software, C.Z. and H.W.; Supervision, F.J.; Validation, X.C.; Writing—original draft, F.N. and H.W.; Writing—review and editing, F.J. and C.Z. All authors have read and agreed to the published version of the manuscript.

Funding: This research was funded by National Natural Science Foundation of China (No. 52274171), the University Synergy Innovation Program of Anhui Province (No. GXXT-2021-018), National Key R&D Program of China (No. 2022YFC2503201), Open Research Grant of Joint National–Local Engineering Research Centre for Safe and Precise Coal Mining (No. EC2023015), and Youth Science and Technology Talents Support Program (2020) by Anhui Association for Science and Technology (No. RCTJ202005).

Data Availability Statement: The data presented in this study are available on request from the corresponding author. The data are not publicly available due to privacy.

Conflicts of Interest: The authors declare no conflict of interest.

References

1. Yuan, L. Innovation and development of safety science and technology in coal industry of China. *Saf. Coal Mines* **2015**, *46*, 5–11.
2. Zheng, C.; Chen, Z.; Kizil, M.; Aminossadati, S.; Zou, Q.; Gao, P. Characterisation of mechanics and flow fields around in-seam methane gas drainage borehole for preventing ventilation air leakage: A case study. *Int. J. Coal Geol.* **2016**, *162*, 123–138. [CrossRef]
3. Xue, S.; Zheng, C.; Kizil, M.; Jiang, B.; Wang, Z.; Tang, M.; Chen, Z. Coal permeability models for enhancing performance of clean gas drainage: A review. *J. Pet. Sci. Eng.* **2021**, *199*, 108283. [CrossRef]
4. Zheng, C.; Jiang, B.; Xue, S.; Chen, Z.; Li, H. Coalbed methane emissions and drainage methods in underground mining for mining safety and environmental benefits: A review. *Process Saf. Environ. Prot.* **2019**, *127*, 103–124. [CrossRef]
5. Pan, Z.; Connell, L.D. Modelling permeability for coal reservoirs: A review of analytical models and testing data. *Int. J. Coal Geol.* **2012**, *92*, 1–44. [CrossRef]
6. Chen, Z.; Liu, J.; Pan, Z.; Connell, L.D.; Elsworth, D. Influence of the effective stress coefficient and sorption-induced strain on the evolution of coal permeability: Model development and analysis. *Int. J. Greenh. Gas Control* **2012**, *8*, 101–110. [CrossRef]
7. Liu, J.; Chen, Z.; Elsworth, D.; Qu, H.; Chen, D. Interactions of multiple processes during CBM extraction: A critical review. *Int. J. Coal Geol.* **2011**, *87*, 175–189. [CrossRef]
8. Yang, X.; Tao, Z.; Cai, B.; Lu, Y. Numerical simulation on fluid-solid coupling of gassy coal and rock. *J. Liaoning Tech. Univ. (Nat. Sci.)* **2014**, *33*, 1009–1014.
9. Zhang, W.; Xu, K.; Lei, Y. Numerical Simulation of the Flow Solid Coupling Effect in the Seam Roadway Pre-exhaust Gas Zone. *J. Northeast. Univ. (Nat. Sci.)* **2017**, *38*, 1628.
10. Fan, C.; Li, S.; Zhang, H.; Yang, Z. Rational boreholes arrangement of gas extraction from unloaded coal seam. *Adv. Civ. Eng.* **2018**, *2018*, 1501860. [CrossRef]
11. Xu, K.; Wang, B.; Liu, Q. Study on gas drainage radius and distance between boreholes based on dynamic fluid-solid coupling model. *Coal Sci. Technol.* **2018**, *46*, 102–108.
12. Yang, X.; Gong, T.; Su, C.; Li, W. Numerically simulated investigation for the thermal migration regularity of CBM in the process of heat injection exploitation under the gas-solid coupling condition. *J. Saf. Environ.* **2021**, *21*, 1551–1558.
13. Liu, J.; Chen, Z.; Elsworth, D.; Miao, X.; Mao, X. Linking gas-sorption induced changes in coal permeability to directional strains through a modulus reduction ratio. *Int. J. Coal Geol.* **2010**, *83*, 21–30. [CrossRef]
14. Shang, Y.; Wu, G.; Kong, D.; Wang, Y.; Li, F. Research on Influencing Factors of Effective Gas Extraction Radius in Coal Mine Based on Multiple Linear Regression. *Adv. Mater. Sci. Eng.* **2022**, 1–13. [CrossRef]
15. Liang, B.; Yuan, X.; Sun, W. Seepage coupling model of in-seam gas extraction and its applications. *J. China Univ. Min. Technol.* **2014**, *43*, 208–213.
16. Liu, Q.; Cheng, Y.; Zhou, H.; Guo, P.; An, F.; Chen, H. A mathematical model of coupled gas flow and coal deformation with gas diffusion and Klinkenberg effects. *Rock Mech. Rock Eng.* **2015**, *48*, 1163–1180. [CrossRef]
17. Liu, Q.; Cheng, Y.; Haifeng, W.; Hongxing, Z.; Liang, W.; Wei, L.; Hongyong, L. Numerical assessment of the effect of equilibration time on coal permeability evolution characteristics. *Fuel* **2015**, *140*, 81–89. [CrossRef]
18. Li, S.; Zhang, H.; Fan, C.; Bi, H.; Yang, Z.; Tao, M. A flow-solid coupling model considering matrix methane seepage for coal methane extraction. *China Saf. Sci. J.* **2018**, *28*, 114–119.
19. Qin, Y.; Liu, P.; Liu, W.; Hao, Y.; Yang, Y.; He, C. Modeling and numerical simulation of borehole methane flow in a dual-porosity, dual-permeability coal seam. *J. China Univ. Min. Technol.* **2016**, *45*, 1111–1117.
20. Wei, M.; Liu, J.; Feng, X.; Wang, C.; Fang, K.; Zhou, F.; Zhang, X.; Xia, T. Quantitative study on coal permeability evolution with consideration of shear dilation. *J. Nat. Gas Sci. Eng.* **2016**, *36*, 1199–1207. [CrossRef]
21. Danesh, N.N.; Chen, Z.; Aminossadati, S.M.; Kizil, M.S.; Pan, Z.; Connell, L.D. Impact of creep on the evolution of coal permeability and gas drainage performance. *J. Nat. Gas Sci. Eng.* **2016**, *33*, 469–482. [CrossRef]
22. Zhang, S.; Liu, J.; Wei, M.; Elsworth, D. Coal permeability maps under the influence of multiple coupled processes. *Int. J. Coal Geol.* **2018**, *187*, 71–82. [CrossRef]
23. Liu, T.; Lin, B.; Yang, W.; Zhai, C.; Liu, T. Coal permeability evolution and gas migration under non-equilibrium state. *Transp. Porous Media* **2017**, *118*, 393–416. [CrossRef]
24. Chen, Z.; Liu, J.; Elsworth, D.; Pan, Z.; Wang, S. Roles of coal heterogeneity on evolution of coal permeability under unconstrained boundary conditions. *J. Nat. Gas Sci. Eng.* **2013**, *15*, 38–52. [CrossRef]
25. An, F.; Cheng, Y.; Wang, L.; Li, W. A numerical model for outburst including the effect of adsorbed gas on coal deformation and mechanical properties. *Comput. Geotech.* **2013**, *54*, 222–231. [CrossRef]
26. Yang, D.; Qi, X.; Chen, W.; Wang, S.; Dai, F. Numerical investigation on the coupled gas-solid behavior of coal using an improved anisotropic permeability model. *J. Nat. Gas Sci. Eng.* **2016**, *34*, 226–235. [CrossRef]
27. Li, S.; Fan, C.; Han, J.; Luo, M.; Yang, Z.; Bi, H. A fully coupled thermal-hydraulic-mechanical model with two-phase flow for coalbed methane extraction. *J. Nat. Gas Sci. Eng.* **2016**, *33*, 324–336. [CrossRef]
28. Liu, T.; Lin, B.; Yang, W.; Liu, T.; Kong, J.; Huang, Z.; Wang, R.; Zhao, Y. Dynamic diffusion-based multifield coupling model for gas drainage. *J. Nat. Gas Sci. Eng.* **2017**, *44*, 233–249. [CrossRef]
29. Zhang, H.; Liu, J.; Elsworth, D. How sorption-induced matrix deformation affects gas flow in coal seams: A new FE model. *Int. J. Rock Mech. Min. Sci.* **2008**, *45*, 1226–1236. [CrossRef]

30. Wu, Y.; Liu, J.; Elsworth, D.; Miao, X.; Mao, X. Development of anisotropic permeability during coalbed methane production. *J. Nat. Gas Sci. Eng.* **2010**, *2*, 197–210. [CrossRef]
31. Fan, C.; Li, S.; Lan, T.; Yang, Z.; Luo, M.; Tao, M. Influence of coal permeability anisotropy on in-seam borehole gas extraction. *China Saf. Sci. J.* **2017**, *27*, 132–137.
32. Duan, M.; Jiang, C.; Gan, Q.; Zhao, H.; Yang, Y.; Li, Z. Study on permeability anisotropy of bedded coal under true triaxial stress and its application. *Transp. Porous Media* **2020**, *131*, 1007–1035. [CrossRef]
33. Liu, T.; Lin, B.; Fu, X.; Zhao, Y.; Gao, Y.; Yang, W. Modeling coupled gas flow and geomechanics process in stimulated coal seam by hydraulic flushing. *Int. J. Rock Mech. Min. Sci.* **2021**, *142*, 104769. [CrossRef]
34. Li, S.; Zhang, H.; Fan, C.; Tao, M. Coal seam dual media model and its application to the proper interpolation among the boring-holes in gas extraction. *J. Saf. Environ.* **2018**, *18*, 1284–1289.